Available online at www.sciencedirect.com
SCIENCE DIRECT®
Composites Science and Technology 63 (2003) 1591–1598
COMPOSITES SCIENCE AND TECHNOLOGY
www.elsevier.com/locate/compscitech

Preparation and characterization of metal oxide/polyimide nanocomposites☆

Craig. M. Thompson*,[1], Helen M. Herring[2], Thomas S. Gates, John. W. Connell

National Aeronautics and Space Administration (NASA), Langley Research Center (LaRC), Hampton, VA 23681-2199, USA

Received 24 August 2002; received in revised form 16 September 2002; accepted 15 December 2002

Abstract

In an effort to introduce low levels of electrical conductivity into space durable polyimides while maintaining optical clarity, nanocomposites containing metal oxides were prepared and characterized. Polymeric materials that exhibit space environmental durability, high optical transmission, low solar absorptivity and sufficient electrical conductivity for electrostatic charge dissipation are needed for future ultra-lightweight, deployable spacecraft. Samples were prepared by the addition of the metal oxide to a pre-made polyimide solution and by the synthesis of the polyimide in the presence of the metal oxide. Sonication was used to aid in the dispersion of the metal oxide particles in *N,N*-dimethylacetamide prior to mixing. Thin films were prepared and characterized for thermal and mechanical properties, solar absorptivity, thermal emissivity, electrical conductivity, optical transmission and degree of dispersion of the metal oxide particles. The effect of the metal oxide particles on the polyimide properties will be discussed.
Published by Elsevier Ltd.

Keywords: Space environmentally durable polyimides; Nanocomposites; Metal oxides

1. Introduction

Future space mission concepts involving large ultra-lightweight (i.e. "Gossamer") spacecraft are actively being pursued by several Government Agencies in the United States and abroad [1]. Gossamer spacecraft are envisioned to be fabricated from flexible, compliant materials that can be folded or packaged into small volumes commensurate with those available on conventional launch vehicles. Upon achieving orbit, the Gossamer structure would be deployed by mechanical, inflation or other means into a large ultra-lightweight functioning spacecraft. Gossamer spacecraft offer a significant cost advantage compared to on-orbit construction and the large size can enable some unique missions. Examples of Gossamer spacecraft include solar sails, antennae, sunshields, rovers, radars, solar concentrators, and reflector arrays. Mission concepts for Gossamer spacecraft encompass a variety of orbits from low Earth orbit (LEO) to the second Lagrangian point (L2) and beyond. Materials represent one of several technologies needed to enable Gossamer spacecraft. The materials used to fabricate Gossamer spacecraft must possess, and maintain, a specific and unique combination of properties over long periods in a relatively harsh environment. The materials must be resistant to the radiation and thermal conditions present in the desired spacecraft location and, depending upon the function of the spacecraft, must possess a combination of mechanical, electrical and optical properties as well. In most applications, sufficient electrical conductivity to mitigate static charge build-up is a necessity. Other desirable properties that are common among many of the mission concepts include low solar absorptivity (α), high thermal emissivity (ε), high optical transparency, toughness, tear and wrinkle resistance. Also the ability to be folded, seamed, bonded to, melt or solution processed into precise shapes is important. Thus the challenge is to

* Corresponding author.
E-mail address: c.m.thompson@larc.nasa.gov (C.M. Thompson).
[1] National Research Council Research Associate
[2] Lockheed Martin Space Operations

0266-3538/03/$ - see front matter Published by Elsevier Ltd.
doi:10.1016/S0266-3538(03)00062-9

incorporate all of the desired properties into a single material.

Metal oxides have been incorporated into polymers as a means of altering electrical and other properties while attempting to maintain high optical transmission [2–8]. In particular, conductive metal oxides such as indium tin oxide and antimony tin oxide have been used to achieve electrical conductivity while maintaining optical transparency and some degree of flexibility. Other approaches have used a multi-layer method whereby thin layers (~50 nm) of conductive materials are deposited onto a plastic substrate. Using this approach, surface resistances of less than 16 ohm/square with 80% transmittance at 550 nm have been achieved [9]. In the work reported herein, indium tin oxide and antimony tin oxide of nanometer particle size were mixed into space durable polymers in an attempt to impart low levels of conductivity to the materials without degrading other desirable properties such as optical transparency. Several different dispersing methods were investigated. Yttrium oxide (an insulator) particles of nanometer dimensions were also used as a means to investigate its dispersion characteristics and their effect on mechanical properties relative to the conductive metal oxide nanometer particles. Thin films were prepared, characterized and tested for thermal, optical, electrical and mechanical properties. Results from these tests will be provided and the relative differences in material behavior will be highlighted.

2. Experimental

2.1. Starting materials

Oxydiphthalic dianhydride (ODPA, Imitec Inc., m.p. 224–225.5 °C) and 1,3-bis(3-aminophenoxy)benzene (APB, Mitsui Chemicals America, Inc., m.p. 107–108.5 °C) were used as received. 4,4′-Perfluoroisopropyidiene dianhydride (6FDA, m.p. 241–243 °C) was sublimed and [2,4-bis(3-aminophenoxy)-phenyl]diphenylphosphine oxide (3-APPO, m.p. 195–197 °C) was prepared as previously reported [10]. NanoTek® antimony tin oxide (ATO, average particle size 11–29 nm, specific surface area 30–80 m^2/g), NanoTek® indium tin oxide (ITO, average particle size 17-30 nm, specific surface area 40–70 m^2/g), and NanoTek® yttrium oxide (average particle size 11–44 nm, specific surface area 19-80 m^2/g) were purchased from Nanophase Technologies Corporation and used as-received. All other chemicals were used as received from commercial sources.

2.2. Characterization

Differential scanning calorimetry (DSC) was conducted on a Shimadzu DSC-50 thermal analyzer. Glass transition temperatures (T_g) were determined at 20 °C/min and were taken as the inflection point of the ΔT vs. temperature curve. Dynamic thermogravimetric analyses (TGA) were performed on a Seiko Model 200/220 instrument on film samples at a heating rate of 2.5 °C/min in air and nitrogen at a flow rate of 15 cm^3/min. Thermal emissivities (ε) were measured on thin film samples using an AZ Technology TEMP 2000A infrared reflectometer. Solar absorptivities (α) were measured on an AZ Technology Model LPSR 300 spectroreflectometer with measurements taken between 250 and 2800 nm with a vapor deposited aluminum on Kapton® film (1st surface mirror) as a reflective reference for air mass 0 per ASTM E903. Ultraviolet/visible (UV/vis) spectroscopy was performed on thin films using a Perkin-Elmer Lambda 900 UV/VIS/NIR spectrometer. Dynamic mechanical analysis (DMA) was performed using a Thermal Analysis 2980 dynamic mechanical analyzer with a tension film clamp installed. The film samples were cut to be between 5 and 6.5 mm in width and 20 and 30 mm in length to conform to the dimensional limits required for the tension film clamp. The average thickness for each film sample was based on three separate measurements at the two ends and the middle of the specimen with a Starrett Model 734 Electronic Digital Micrometer. After mounting the sample in the DMA, the test procedure consisted of cooling the film sample to −120 °C, holding for 5 min, and then heating at 3 °C/min to 250 °C under a preload of 0.5 N, a single frequency of 1 Hz, and an amplitude of 20 μm. At least three separate tests were run for each distinct film. The storage modulus for each run was found as a function of increasing temperature. Optical microscopy characterization was preformed with a Nikon Eclipse ME600 transmission microscope outfitted with an X–Y translation stage. A Nikon DXM 1200 digital camera was used to record the images. The sample was imaged in the as-received condition at a magnification of 200×.

2.3. Polymer preparation

Two low color, soluble, space durable polyimides, (TOR-NC and LaRC™ CP-2) were prepared by reacting stoichiometric quantities of the diamines with the respective dianhydrides. TOR-NC is derived from ODPA and 3-APPO as previously reported [10]. LaRC™ CP-2 is derived from 6FDA and APB as previously reported [11]. The following procedure is representative for the preparation of either polyimide. A 200 ml three neck round bottom flask fitted with a mechanical stirrer, nitrogen gas inlet, and drying tube filled with calcium sulfate was charged with APB (5.8481 g, 0.0200 mol) and 8 ml of *N,N*-dimethylacetamide (DMAc). A slurry of 6FDA (8.9288 g, 0.0200 mol) in 10 ml of DMAc was prepared and added to the diamine solution. An additional 60 ml of DMAc was used to wash in the solids and to prepare a 20% solids (w/w) solution. The light yellow solution was stirred overnight at room temperature under a nitrogen atmosphere. A 0.5% solution in DMAc exhibited an inherent viscosity of 1.35 dl/g at 25 °C. The remaining polymer solution was chemically imidized by the addition of 5.3 ml of acetic anhydride and 4.7 ml of pyridine followed by stirring at room temperature under nitrogen overnight. The polymer was precipitated into a blender containing water, filtered, washed with excess water and dried in a vacuum oven at 100 °C overnight to give a nearly quantitative yield of polyimide.

2.4. Nanocomposite preparation

Nano-scale metal oxides were incorporated into the polyimide matrix either by addition of the materials to previously prepared polymer or by preparing the polymer in the presence of the metal oxide powders. Details of the methods are as follows.

2.4.1. Method A: addition of the metal oxide powder to prepared polymer

Indium tin oxide (0.0520 g) was combined with 8.5 ml of DMAc in a sample vial and the vial was partially immersed in a ultrasonic bath for 90 min. TOR-NC (1.73 g) was added to the mixture and sonication was continued overnight. A film was cast from the suspension on plate glass. The film was dried to a tack-free state in a low humidity chamber followed by drying for 1 h each at 50, 100, 150, 175, and 225 °C in a forced air oven.

2.4.2. Method B: preparation of the polymer in the presence of the metal oxide powder

Indium tin oxide (0.1673 g) and 5 mL of DMAc were combined in a sample vial and sonicated for 15 min. The ITO suspension was transferred to a 100 ml three neck round bottom flask fitted with a mechanical stirrer, nitrogen gas inlet, and drying tube and containing 3-APPO (3.5958 g, 0.0073 mol). The ITO suspension was washed into the flask with 5 ml of DMAc. A slurry of ODPA (2.2647 g, 0.0073 mol) in 5 ml of DMAc was prepared and added to the flask. An additional 10 ml of DMAc was used to wash in all solids and create a solution of 20% (w/w) solids. The suspension was stirred overnight at room temperature under nitrogen. The poly(amide acid) was chemically imidized through the addition of acetic anhydride (2.2 ml) and pyridine (1.8 ml) followed by stirring overnight. A film was cast from the suspension on plate glass. The film was dried to a tack-free state in a low humidity chamber followed by drying for 1 hour each at 50, 100, 150, 175, and 225 °C in a forced air oven.

2.5. Films

Thin films were cast from polyimide-metal oxide suspensions in DMAc. The mixtures were cast using a doctor blade onto clean, dry plate-glass and dried to a tack-free form in a low humidity chamber. The films then were treated in a forced air oven staged to 225 °C for 1 h.

2.6. Film tensile properties

Thin-film tensile properties (elastic modulus, strength, elongation at break) were determined according to ASTM D882 using four or five specimens (0.51 cm wide) per material type. Average values along with the calculated standard deviation are reported. Tests were performed at room temperature using a Sintech 2 screw driven test frame with a 11.4 kg load cell. The test specimen gauge length was 5.1 cm and the crosshead speed for the film testing was 0.51 cm/min. Stress was calculated based on the measured load and the average film cross section measured prior to loading. After initial loading to remove any slack in the film, strain was calculated based on measured crosshead movement divided by the starting distance between the grips.

2.7. Conductivity measurements

Conductivity measurements were performed on thin films following the general procedure described in ASTM D257 using a Keithley 8009 Resistivity Test Fixture and a Keithley 6517 Electrometer.

3. Results and discussion

3.1. Nanocomposite preparation

Two low color, soluble polyimides that have exhibited good resistance to UV and electron radiation, and in the case of TOR-NC, atomic oxygen resistance, were selected for use in this study. TOR-NC is a low color, soluble polyimide that has exhibited excellent resistance to UV degradation and electron radiation. In addition, it exhibits one to two orders of magnitude improved resistance to atomic oxygen as compared to Kapton® HN polyimide [10]. LaRC™ CP-2 is a low color, soluble polyimide that has exhibited excellent UV and electron radiation resistance [12]. The synthesis of TOR-NC and LaRC™ CP-2 are depicted in Scheme 1. Nanocomposites were prepared by the dispersion of antimony tin oxide, indium tin oxide, and yttrium oxide nano-scale powders (~10–44 nm) into these two polyimides. The composites were prepared at an ~3% (w/w) loading either through direct addition of the metal oxide powders to pre-made polyimide (Method A), or through preparing the polyimide in the presence of the metal oxide powders (Method B). A loading of 3% (w/w) was chosen based on preliminary screening where it was observed that higher loading levels embrittled the

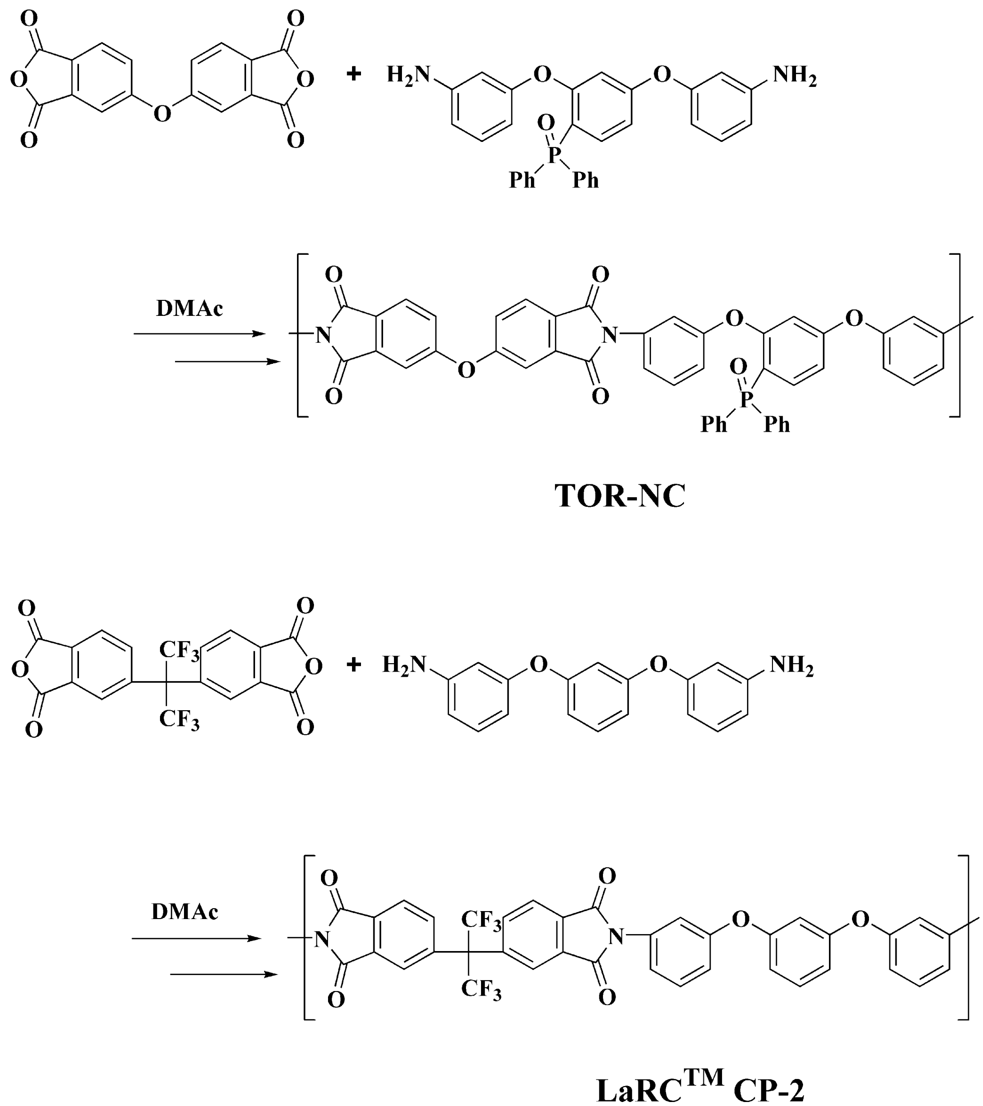

Scheme 1. Synthesis of TOR-NC and LaRC™ CP-2.

materials. It was anticipated that lower loading levels would not reach the percolation threshold.

Method A involved dispersing the metal oxide powders in DMAc with sonication followed by addition of solid polymer and more solvent to make an ~20% (w/w) solids–polymer solutions. The mixtures were placed in an ultrasonic water bath operating at 40 kHz at ambient temperature. The polymer-powder mixtures were sonicated overnight. During this time, the water bath temperature increased to the 40–50 °C range. The resulting suspensions were cast onto plate glass in a dry-air chamber. After drying to a tack-free state, the films on glass were thermally treated for 1 h each at 50, 100, 150, 175 and 225 °C. The thin films were subsequently removed from the glass and characterized.

Method B involved synthesizing the polyimide in the presence of pre-dispersed metal oxide powders. The metal oxide powders were placed into DMAc (~3% solids) and sonicated for 15 min. This suspension was subsequently added to a reaction flask containing a DMAc solution of the diamine. The dianhydride was subsequently added as a solid and the mixture was allowed to stir at room temperature (RT) overnight under a nitrogen atmosphere. The resulting viscous poly(amide acid) metal oxide suspension was treated at RT with acetic anhydride/pyridine to cyclodehydrate the poly(amide acid) to form the polyimide. These suspensions were used to cast thin films onto plate glass. The films were dried using the procedure described above for Method A.

In all cases the amount of metal oxide relative to the amount of polyimide in the nanocomposite films was ~3% by weight. In general, good quality films were produced that were similar in appearance but more brittle than the controls. The ATO containing films had a light blue color and the ITO films were pale yellow. Sample 3B as defined in Table 1 (TOR–NC–Y_2O_3) gave films that were very brittle and could not be removed from the glass

Table 1
Thermal properties of polymer-metal oxide materials

Sample number[a]	Polymer	Additive	T_g [b], (°C)	TGA[c] 5 wt.% loss	
				(N_2)	(Air)
	TOR-NC	None	212	478	461
1A	TOR-NC	ATO	210	472	465
1B	TOR-NC	ATO	203	478	476
2A	TOR-NC	ITO	202	459	468
2B	TOR-NC	ITO	197	474	464
3A	TOR-NC	Y_2O_3	196	465	461
3B	TOR-NC	Y_2O_3	209	431	413
	LaRC™ CP-2	None	203	461	456
4A	LaRC™ CP-2	ATO	192	494	485
4B	LaRC™ CP-2	ATO	194	490	483
5A	LaRC™ CP-2	ITO	195	498	490
5B	LaRC™ CP-2	ITO	200	502	488
6A	LaRC™ CP-2	Y_2O_3	189	498	473
6B	LaRC™ CP-2	Y_2O_3	206	473	429

[a] A = Metal oxide powder added to polymer solution. B = Polymer prepared in the presence of the metal oxide powder.
[b] Determined on thin film by DSC at a heating rate of 10 °C/min.
[c] Determined on thin films at a heating rate of 2.5 °C/min.

Table 2
Room temperature thin-film tensile properties

Sample number[a]	Polymer	Additive	Tensile strength (MPa)		Tensile modulus (GPa)		Elong. @ break%	
			Avg.	S.D.	Avg.	S.D.	Avg.	S.D.
	TOR-NC	–	97.00	–	2.80	–	5.0	–
1A	TOR-NC	ATO	66.47	30.55	3.16	0.22	2.5	1.4
1B	TOR-NC	ATO	93.93	7.52	3.19	0.07	3.7	0.4
2A	TOR-NC	ITO	112.34	5.33	3.25	0.06	5.2	0.5
2B	TOR-NC	ITO	90.17	7.76	3.36	0.18	3.3	0.2
3A	TOR-NC	Y_2O_3	111.86	8.94	3.39	0.05	4.7	0.7
	LaRC™ CP-2	–	115.00	–	2.90	–	6.0	–
4A	LaRC™ CP-2	ATO	109.50	3.78	3.53	0.26	4.3	0.8
4B	LaRC™ CP-2	ATO	114.62	4.69	3.29	0.12	4.8	0.1
5A	LaRC™ CP-2	ITO	107.82	4.20	3.26	0.10	4.6	0.2
5B	LaRC™ CP-2	ITO	110.61	10.45	3.23	0.12	4.5	0.6
6A	LaRC™ CP-2	Y_2O_3	105.90	4.71	3.27	0.05	4.4	0.4
6B	LaRC™ CP-2	Y_2O_3	90.24	9.32	2.98	0.11	3.9	0.8

[a] A = Metal oxide powder added to polymer solution. B = Polymer prepared in the presence of the metal oxide powder.

plate without fracturing whereas sample 3A gave good quality films. The TOR–NC–Y_2O_3 solution (sample 3B) appeared visually to be high molecular weight based upon the apparently high solution viscosity. Inherent viscosity measurements were not performed due to the presence of the metal oxide powders.

3.2. Characterization

Thermal properties of the nanocomposite films are presented in Table 1. The TOR–NC nanocomposite films exhibited T_gs from 196 to 210 °C, slightly lower than the control which had a T_g of 212 °C. In comparing similar samples prepared by Method A and B, films prepared by Method A containing ATO or ITO exhibited higher T_gs. The TOR–NC–Y_2O_3 films exhibited the opposite trend. The LaRC™ CP-2 nanocomposite films exhibited T_gs from 189 to 206 °C, in most cases slightly lower than the control (T_g = 202 °C). Metal oxide containing films of LaRC™ CP-2 prepared by method B all exhibited higher T_gs then analogous samples prepared by method A. The samples exhibited temperatures of 5% weight loss ranging from 413 to 490 °C in air, in most cases slightly higher than that of the control. In nitrogen, the temperatures of 5% weight loss ranged from 431 to 502 °C.

3.3. Thin film tensile properties

Room temperature thin film tensile properties are presented in Table 2. The TOR–NC and the LaRC™ CP-2 films (with additives) exhibited comparable strengths to the respective controls, however the TOR–NC films had a wider scatter about the baseline value and in general had higher standard deviations for each sample type. In particular, sample 1A had a standard deviation exceeding 30 MPa. The tensile modulus for both the TOR–NC and LaRC™ CP-2 films fell within a narrow range with little difference due to material type. In general, the films with additives exhibited comparable or lower strengths and elongations compared to the baseline. The moduli for all nanocomposite films were higher than that of the control.

3.4. Dynamic mechanical analyses

Figs. 1 and 2 are composite graphs of temperature versus the storage modulus for each film, tested using DMA. Each film is represented by a single curve, considered typical of its test runs. In Fig. 1, a distinct separation in the storage modulus was shown between the A and B classes of films. The storage modulus of the clean (control) polymer film fell in between these two classes. In Fig. 2, however, the storage modulus fell lower than that of the clean (control) polymer for all films but one.

Table 3 shows the average storage modulus and standard deviation for each film sample at four specific temperatures in the test run. The scatter in the values is due to non-uniform thickness of the film samples and DMA instrument thermal instability at very low temperatures.

3.5. Optical transparency

The optical transparency or % light transmission through the film was measured using UV/Vis spectroscopy at 500 nm (the solar maximum) and presented in

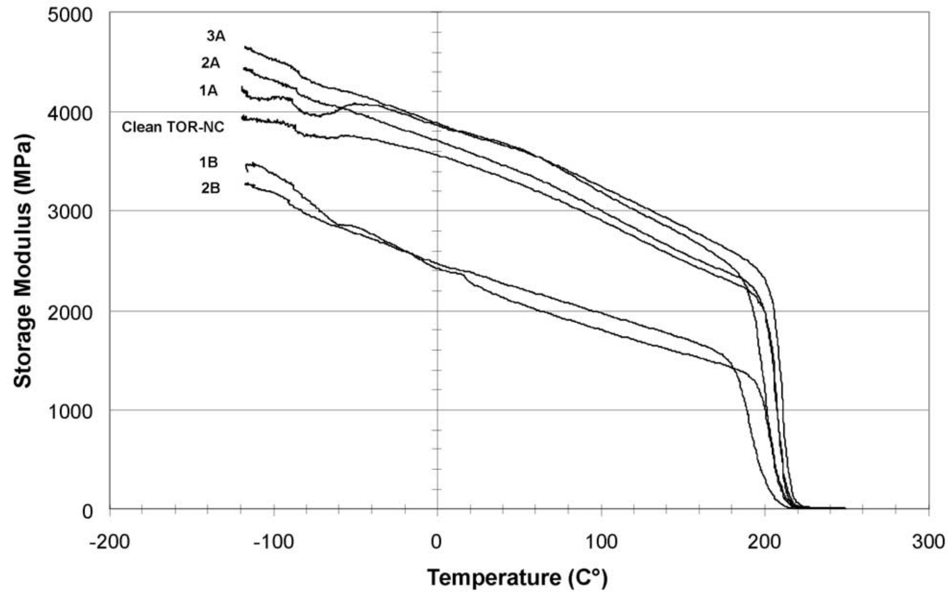

Fig. 1. Temperature versus storage modulus for TOR–NC/metal oxide nanocomposites.

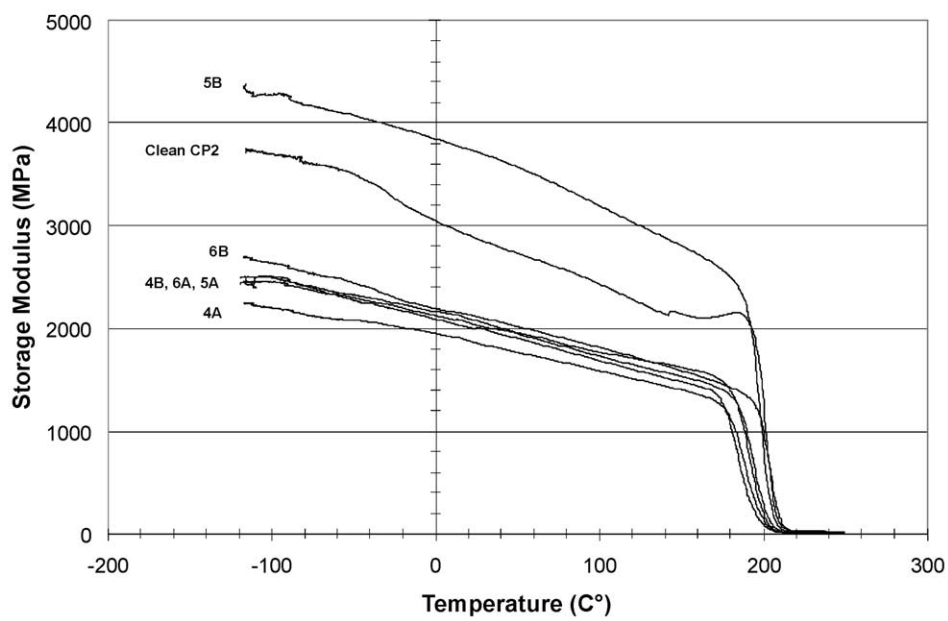

Fig. 2. Temperature versus storage modulus for LaRC^{TM} CP-2/metal oxide nanocomposites.

Table 4. The values ranged from 49 to 77% with film thickness ranging from 0.043 to 0.071 mm. The films were all slightly colored because of the metal oxide additive thus the %T values were all lower then those of the neat polymer. There appeared to be no correlation between the different additives and the drop in %T compared to the neat polymer.

3.6. Optical microscopy

A typical micrographic image of a film sample is shown in Fig. 3. The image shows agglomerates of the metal oxide additive randomly distributed throughout the polymer film.

3.7. Solar absorptivity and thermal emissivity

Two properties important for materials for space applications are solar absorbance (α) and thermal emittance (ε). Solar absorptivity pertains to the fraction of incoming solar energy that is absorbed by the film and solar emissivity is a measure of the films ability to radiate energy from the film surface. Typically a slightly colored film exhibits a low α value. The α and ε values

Table 3
Average storage modulus (MPa)

Sample	−100 °C		23 °C		100 °C		150 °C	
	Avg.	S.D.	Avg.	S.D.	Avg.	S.D.	Avg.	S.D.
Clean TOR-NC	4078.7	273.2	3200.0	308.4	2636.8	318.3	2255.7	269.5
1A	4101.0	250.4	3394.3	592.0	2901.7	488.1	2552.1	399.2
1B	3404.8	722.7	2626.2	865.1	2190.3	767.6	1919.6	667.5
2A	3399.8	332.6	2750.6	920.7	2392.1	724.7	2094.3	606.9
2B	2859.6	284.3	2167.0	183.7	1812.0	162.9	1588.3	147.0
3A	4297.4	540.8	3418.3	512.5	2846.7	458.0	2441.8	384.2
Clean LaRC™ CP-2	3178.7	539.0	3006.4	205.3	2565.9	189.6	2236.3	147.4
4A	2210.0	11.2	1809.8	50.2	1521.8	55.5	1350.5	44.0
4B	2716.1	241.2	2108.8	183.6	1699.8	56.3	1487.6	45.6
5A	2529.4	364.7	2117.1	107.9	1782.9	53.7	1592.3	53.3
5B	4150.0	612.7	3735.8	11.7	3185.1	8.0	2792.9	10.0
6A	2455.1	278.7	1932.2	135.1	1621.4	98.5	1438.9	85.2
6B	2898.6	734.6	1977.0	134.4	1746.9	128.7	1519.2	93.5

Table 4
Solar absorbance (α), thermal emittance (ϵ) and optical transparency of thin-films

Sample number[a]	Polymer	Additive	Sample thickness (mm)	%T (500 nm)	α	ε	α/ε
	TOR-NC	None	0.041	85	0.05	0.56	0.09
1A	TOR-NC	ATO	0.053	69	0.19	0.79	0.24
1B	TOR-NC	ATO	0.046	65	0.17	0.78	0.22
2A	TOR-NC	ITO	0.046	68	0.17	0.82	0.21
2B	TOR-NC	ITO	0.071	49	0.20	0.83	0.24
3A	TOR-NC	Y_2O_3	0.043	77	0.08	0.66	0.12
	LaRC™ CP-2	None	0.028	89	0.05	0.45	0.11
4A	LaRC™ CP-2	ATO	0.051	67	0.22	0.77	0.29
4B	LaRC™ CP-2	ATO	0.048	54	0.21	0.75	0.28
5A	LaRC™ CP-2	ITO	0.051	68	0.19	0.78	0.24
5B	LaRC™ CP-2	ITO	0.048	52	0.17	0.77	0.22
6A	LaRC™ CP-2	Y_2O_3	0.043	68	0.08	0.61	0.13
6B	LaRC™ CP-2	Y_2O_3	0.046	60	0.12	0.62	0.19

[a] A = metal oxide powder added to polymer solution. B = polymer prepared in the presence of the metal oxide powder.

for the thin films containing the metal oxide particles are shown in Table 4. Alpha values ranged from 0.08 to 0.22 and ε values ranged from 0.61 to 0.83. Ideal values for many space applications are less than 0.1 for α and greater than 0.6 for ε. In all cases the addition of the metal oxide nanopowders to the polyimides increased both α and ε relative to the parent polymers.

3.8. Conductivity measurements

Surface and volume conductivities were measured on selected nanocomposite film specimens and are presented in Table 5. In all cases there was a slight increase in surface conductivity of about two orders of magnitude. A

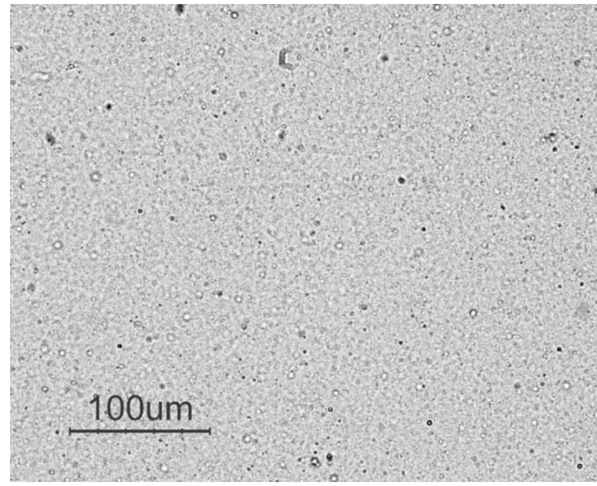

Fig. 3. Optical micrograph of sample 5B.

Table 5
Conductivity measurements on thin-films

Sample number[a]	Polymer	Additive	Surface conductivity, (S)	Volume Conductivity, (S/cm)
	TOR-NC	None	0.2×10^{-14}	1×10^{-16}
1A	TOR-NC	ATO	0.5×10^{-12}	0.3×10^{-10}
1B	TOR-NC	ATO	0.3×10^{-13}	0.1×10^{-14}
2A	TOR-NC	ITO	0.2×10^{-12}	0.2×10^{-14}
2B	TOR-NC	ITO	0.1×10^{-11}	0.2×10^{-13}
	LaRC™ CP-2	None	ND[b]	ND
4A	LaRC™ CP-2	ATO	3.0×10^{-12}	ND
4B	LaRC™ CP-2	ATO	$>1.0\times10^{-12}$	ND
5A	LaRC™ CP-2	ITO	2.9×10^{-12}	ND
5B	LaRC™ CP-2	ITO	$>1.0\times10^{-12}$	ND
6A	LaRC™ CP-2	Y_2O_3	2.6×10^{-12}	ND
6B	LaRC™ CP-2	Y_2O_3	$>1.0\times10^{-12}$	ND

[a] A = metal oxide powder added to polymer solution. B = polymer prepared in the presence of the metal oxide powder.
[b] ND = Not determined.

similar trend was observed for the volume conductivities. The measured conductivities all fell well short of the desired values for electrostatic discharge, which are 10^{-6}–10^{-8} S/cm^2. The poor dispersion of the metal oxide particles within the polymer matrix left large gaps, which hinder charge transport. Also, at the degree of dispersion achieved for these samples, it is unlikely that the percolation threshold was achieved. This is further supported by the observation that the non-conductive additive gave similar results as compared to the conductive additives.

4. Summary and conclusions

Nanocomposite film samples were prepared from three metal oxide powders (ATO, ITO, Y_2O_3) and two space durable polyimides (TOR–NC, LaRC™ CP-2) by two different synthesis methods. The materials were characterized for thermal, electrical, mechanical and optical properties. For most cases, the use of nano-scale additives resulted in films with comparable or lower strengths and elongations and higher stiffness as compared to the baseline polymer. However, in general, the use of nano-scale metal oxide additives lowered the dynamic stiffness (storage modulus) for both polymer types. Processing of the nanocomposite films also influenced the dynamic stiffness over a wide temperature range. This mechanical behavior is typical for what is expected by the addition of a micron-sized filler to a polymer matrix. The drop in strength and elongation to break suggest that dispersion of the metal oxides on a nanometer scale was not achieved. Optical imaging of the films confirms this lack of uniform dispersion and it is assumed that the poor dispersion of the metal oxide particles within the polymer matrix left large gaps, which in turn hindered charge transport. Measured conductivities were well below the desired values for electrostatic discharge. At the degree of dispersion achieved for these samples, it is unlikely that the percolation threshold was achieved. The use of nano-scale metal oxide additives caused an increase in α and ϵ and a decrease in optical transparency. Basic thermal properties (T_g and weight loss) of all the films were similar with no clear trends apparent due to changes in polymer type or processing method. These trends are similar to results reported on the addition of single wall carbon nanotubes to these types of polymers [13–15].

The use of trade names of manufacturers does not constitute an official endorsement of such products or manufacturers, either expressed or implied, by the National Aeronautics and Space Administration.

Acknowledgements

The authors would like to acknowledge Dr. Zoubeida Ounaies for the conductivity measurements on the thin films.

References

[1] Jenkins CHM. Gossamer spacecraft: membrane and inflatable structures technology for space applications, vol. 191. American Institute of Aeronautics and Astronautics; 2001.

[2] Arney DS, Wood TE. Nanosize metal oxide particles for producing transparent metal oxide colloids and creamers, US Patent 6,329,058. Issued December 11, 2001 to 3M Innovative Properties.

[3] Li Y, Tong Y, Jing K, Ding M. Preparation of polyimide $BaTiO_3$ hybrid films by a dispersion process and their microstructure. J Polym Sci (Chinese) 2001;19(1):13–17.

[4] Bian JL, Quian XF, Yin J, Lu QH, Liu L, Zhu Z. Preparation and properties of rare earth oxide/polyimide hybrids. Polym Testing [in press].

[5] Al-Dahoudi N, Bisht H, Gobbert C, Krajewski T, Aegerter MA. Transparent conducting, anti-static and anti-static-anti-glare coatings on plastic substrates. Thin Solid Films 2001;392:299–304.

[6] Chen X, Gonsalves KE. Synthesis and properties of an aluminum nitride/polyimide nanocomposite prepared by a nonaqueous suspension process. J Materials Research 1997;12(5):1274–86.

[7] Liu J., Coleman JP. Nanostructured metal oxides for printed electrochromic displays. 2000;A286:144–8.

[8] Yoshihara M, Oie H, Okada A, Matsui H, Ohshiro S. Synthesis of yttrium-organic hybrid networks. Macromolecules 2002;35: 2435–6.

[9] Fahland M, Karlsson P, Charton C. Low resistivity transparent electrodes for displays on polymer substrates. Thin Solid Films 2001;392:334–7.

[10] Watson KA, Connell JW, Palmieri FL. Space environmentally stable polyimides and copolyimides derived from [2,4-bis(3-aminophenoxy)phenyl]diphenylphosphineoxide. Society of Advanced Materials and Process Engineering Series 2001;46:1853–1863. Macromolecules 2002;35(13):4968–74.

[11] St. Clair AK, St Clair TL, Slemp WS. Optically transparent/colorless polyimides. In: Weber W, Gupta M, editors. Recent advances in polyimide science and technology. Poughkeepsie, NY: Society of Plastics Engineers; 1987. p. 16–36.

[12] Stuckey W, Meshishnek M, Hanna D, Ross F. Space environmental test of materials for inflatable structures. Aerospace Corporation Technical Memorandum 98 (1055-04)-2 1998.

[13] Watson KA, Smith Jr JG, Connell JW. Polyimide/carbon nanotube composite films for potential space applications. Society for the Advancement of Materials and Process Engineering Technical Conference Series 2001;33:1551–60.

[14] Smith Jr JG, Connell JW, Lillihei PT, Watson KA, Thompson CM. Nanocomposite films derived from alkoxysilane terminated amide acid oligomers and carbon nanotubes. Materials Research Society Symposium Proceedings 2002; Paper 51146, T3.5.

[15] Park C, Ounais Z, Watson KA, Crooks RE, Lowther SE, Connell JW, Siochi EJ, Harrison JS, St Clair TL, Smith Jr JG. Dispersion of single wall carbon nanotubes by *in situ* polymerization under sonication. Chemical Physics Letters 2002; 364:303–8.